受 賞 記 事

Pulse Radiolysis Studies of Water and Alcohols at High Temperatures and Supercritical Conditions

Sch. Nucl. Sci. Tech., Univ. Sci. & Tech. China / Institute of Nuclear Energy Safety Technology, CAS
Mingzhang Lin*

In the present article, some studies on the pulse radiolysis of high temperature and supercritical water are summarized. The temperature and density effects on the absorption spectrum of hydrated electron, the yield of water decomposition products, and reaction rate constants are addressed and discussed. Meanwhile, the temperature effects on the absorption spectra of solvated electron at elevated temperatures have been also stated. These investigations are expected to be useful for the modeling of water radiolysis in supercritical water cooled reactors (SCWR) and for a better understanding of fundamental knowledge in radiation chemistry as well.

Keywords: pulse radiolysis, supercritical water, temperature effect, density effect, absorption spectrum

1 Introduction

Despite of its chemical simplicity, water is one of the most important substances on earth. It covers 71 % of our planet's surface and it is vital for all known forms of life. Radiolysis of water was studied soon after the discovery of natural radioactivity. Early researchers starting with Becquerel observed that radium emanations decompose water into hydrogen and oxygen. Thanks to the development of pulse radiolysis techniques, especially the identification of hydrated electron by Hart and Boag in 1962[1)], the reaction mechanism of water radiolysis was then established.

The investigation on water radiolysis is of great interest in biological processes, nuclear power plants, spent fuel reprocessing, nuclear waste repository, etc. Recently, with the development of various technologies, one has been able to investigate water radiolysis under some extreme conditions such as concentrated solutions, high temperature, high pressure, high linear energy transfer (LET), being much closer to some practical applications, especially for the development of advanced nuclear energy systems, where the chemical conditions are usually much more harsh than ever before. Motivated by the R&D needs of supercritical water cooled reactor (SCWR), one of the next generation (GenIV) reactors, we have been involving in the basic studies of water radiolysis at elevated temperatures, especially under supercritical conditions. One of the main purposes is to collect basic data for the computer simulations of water radiolysis in SCWR, so as to have a reasonable water chemistry control at the reactors. As is known, the physico-chemical properties of supercritical water and the water structure (hydrogen bond network) are significantly different from the water at ambient conditions, it is of our great interest to unveil how these changes reflect on the radiolysis of water, such as the yield of water decomposition products, the rate constants, and the properties of chemical species, etc., by using steady irradiation, nanosecond and picosecond pulse radiolysis techniques.

On the other hand, much investigation has been devoted to the pulse radiolysis studies of alcohols, especially the behaviors of solvated electron in those alcohols at elevated temperatures. There are at least two reasons why we are interested in the studies of solvated electrons in high temperature and supercritical alcohols. First, the molecular

Pulse Radiolysis Studies of Water and Alcohols at High Temperatures and Supercritical Conditions
Mingzhang Lin* (*Sch. Nucl. Sci. Tech., Univ. Sci. & Tech. China / Institute of Nuclear Energy Safety Technology, CAS*),
96 Jinzhai Road, Hefei, Anhui 230026, China
TEL&Fax: +86–551–63607732, E-mail: gelin@ustc.edu.cn

structure of simple alcohols such as methanol is similar to that of water while their supercritical conditions are much milder than water, for example, the critical temperature (t_c) and pressure (P_c) of methanol are 239.5 °C and 8.1 MPa, but for H_2O, they are 374 °C and 22.1 MPa, respectively. The investigation is expected to be helpful for a better understanding of the radiolysis of water at elevated temperatures and supercritical water. The second reason is due to the variety and intrinsic properties of alcohols. Structurally, alcohols can have different chain lengths (carbon number) and OH group number. Their polarity (dielectric constant) and viscosity are quite different from those of water and also strongly correlated with the chemical structure. These will eventually affect the solvation processes of electron.

2 Experimental

Most experiments were carried out at the University of Tokyo using an electron linear accelerator coupled with a high temperature high pressure irradiation cell (Taiatsu Techno®). Details of the apparatus for nanosecond pulse radiolysis are described elsewhere[2,3]. The solution was loaded into the cell by an HPLC pump. The temperature of the sample solution was monitored by a thermocouple placed inside the cell and the pressure was adjusted with a back-pressure regulator. The picosecond pulse radiolysis experiments were performed using a photocathode type Linac associated with a femtosecond laser as probe (analyzing) light[4].

3 Results and Discussion

3.1 Absorption spectrum of hydrated electron at elevated temperatures and supercritical water

Typical temperature dependent absorption spectra of e^-_{aq} in D_2O at 25 MPa from room temperature to 380 °C is given in Fig. 1[4]. These absorption spectra are almost the same as those obtained by nanosecond pulse radiolysis. The absorbance decreases with temperature because the water density decreases and the decay of e^-_{aq} is accelerated with increasing temperature. The fact that e^-_{aq} does exist in SCW (t_c = 374 °C, P_c = 22.1 MPa) and even persists at densities as low as $\sim 8 \times 10^{-3}$ g/cm^3 indicates that the electron experiences a strong interaction with the neighboring water molecules, implying a dominant role of the short-range molecular structure in the microscopic description of the electron localization and hydration mechanisms. The plots of absorption maximum (E_{max}) vs. temperature show a monotonic decrease up to subcritical temperature at a fixed pressure.

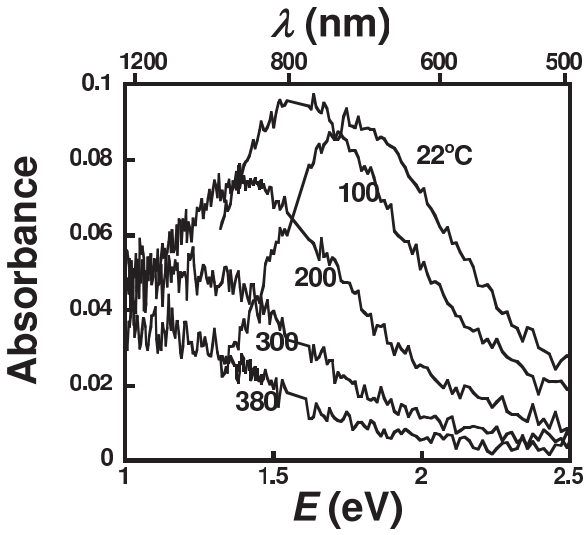

Figure 1. Absorption spectra of hydrated electron obtained by pulse radiolysis of D_2O from room temperature to supercritical state, recording at 60 ps after the electron beam pulse.

Interestingly, the temperature dependence of E_{max} in sub- and supercritical D_2O further reveals that, at a fixed pressure (25 MPa), E_{max} decreases monotonically with increasing temperature in passing through the liquid-SCW phase transition at t_c, but exhibits a minimum at a fixed density (0.2 g/cm^3 and 0.65 g/cm^3) as the water passes above t_c into SCW. These behaviors can be understood by means of simple microscopic arguments based on the changes that occur in the water properties and water structure (clustering) in the sub- and supercritical water regimes. By comparison with the $(H_2O)_n^-$ cluster data obtained at ambient temperature or under cryogenic conditions, the average cluster size in SCW at 400 °C is estimated to be ~32 water molecules for ρ = 0.65 g/cm^3 and ~26 for ρ = 0.2 g/cm^3, respectively[5]. Similar phenomena were observed for the solvated electron in sub- and supercritical methanol[6].

The radical of 4,4′-bipyridyl was also used to probe the local structure of water under sub- and supercritical conditions. The absorption spectra of 4,4′-bpyH$^\bullet$ in various

organic solvents with different dielectric constants were measured at ambient conditions. The absorption maximum E_{max} varied with the solvents used, due to solvent-solute interactions. The plots of E_{max} as a function of the dipolar effect value ($(\epsilon-1)/(\epsilon+2)-(n^2-1)/(n^2+2)$) ($\epsilon$ is dielectric constant and n is refractive index of the solvent) in McRae-Bayliss model[7] show a fairly good linear relationship. However, similar plots for E_{max} of 4,4′-bpyH$^{\bullet}$ under sub- and supercritical conditions remarkably deviate from the line. Further analysis exhibits that there is a local density augmentation for supercritical water, as shown in Fig. 2.

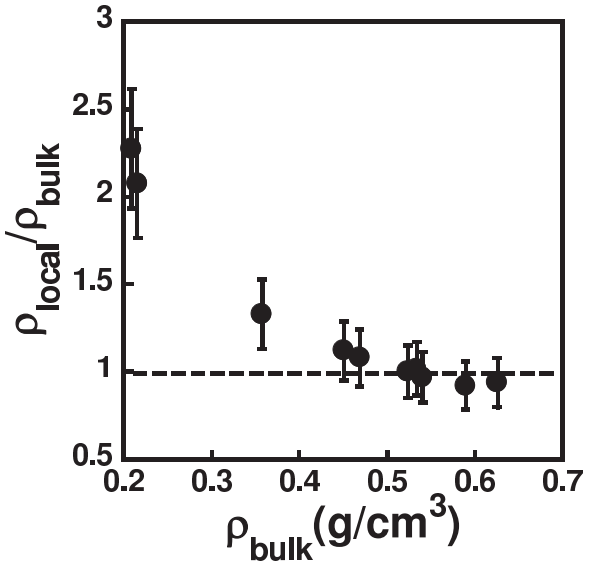

Figure 2. Density enhancement factor as a function of bulk density.

3.2 Radiolytic yield of water decomposition products

$G(e^-_{aq})$ was measured using two scavenging systems: a) methyl viologen (MV^{2+}) in the presence of *tert*-butanol[8], and b) 4,4'-bipyridyl (4,4′-bpy) together with *tert*-butanol in alkaline solution (pH > 11)[9], from 25 °C to 500 °C. For the temperature dependent behaviors at fixed pressure of 25 MPa, $G(e^-_{aq})$ increases with temperature up to 300 °C, and then decreases to a minimum near t_c before jumping to a high value at 400 °C, and then it decreases again with increasing temperature up to 500 °C. An independent measurement of $G(e^-_{sol})$ in methanol shows a similar tendency[10]. The sharp change of $G(e^-_{sol})$ at constant pressure is attributed to density effects. In fact, under supercritical conditions, at a fixed density $G(e^-_{aq})$ decreases with increasing temperature while at a fixed temperature $G(e^-_{aq})$ decreases with increasing water density. Around t_c, the density effect is the most significant, but it becomes less and less as temperature increases. Picosecond pulse radiolysis has been done to confirm the density effect on $G(e^-_{aq})$, Fig. 3[4,11].

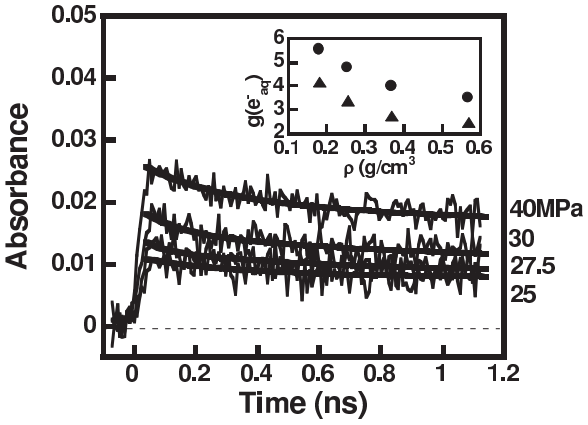

Figure 3. Time profiles for the decay of hydrated electron at 400 °C at different pressures. Inset: yields of hydrated electron at 60 ps and 1 ns as a function of water density.

Two scavenging systems have been used to evaluate $\{G(e^-_{aq}) + G(H^{\bullet}) + G(^{\bullet}OH)\}$ (denoted as G_{sum}). One is 0.5 mM MV^{2+} with 0.2 M ethanol, another is 0.5 mM 4,4′-bpy in the presence of 10 mM HCOONa. The solutions are deaerated by Ar gas. Ethanol and $HCOO^-$ are used to convert OH radical and H atom to ethanol radical and $COO^{\bullet-}$ which will subsequently reduce MV^{2+} and 4,4′-bpy to form $MV^{\bullet+}$ and 4,4′-bpyH, the same as those produced by e^-_{aq}, that is, the total yields of $MV^{\bullet+}$ or 4,4′-bpyH should be equal to the total yield G_{sum}. The tendency is very similar to that of $G(e^-_{aq})$. An estimation of the yield of $COO^{\bullet-}$ up to 400 °C by pulse radiolysis of 10 mM sodium formate in N_2O saturated solution well supported these results[10].

The estimation of $G(^{\bullet}OH)$ has been carried out using an aerated solution of 100 mM $NaHCO_3$ or a deaerated solution of 100 mM $NaHCO_3$ in the presence of 1 mM $NaNO_3$. In these systems, hydrated electrons are scavenged by O_2 or NO_3^- while the reaction between H atoms and HCO_3^- is rather slow. Consequently the yield of $CO_3^{\bullet-}$ would correspond to $G(^{\bullet}OH)$. From room temperature to 380 °C, the

pressure is 25 MPa while at 400 °C it is 35 MPa because the solubility of $NaHCO_3$ at 400 °C/25 MPa is too low to do the measurements.

It is noted that the measurement of *G*-value of water decomposition products is largely related to the concentration of scavenger, or the scavenging time. Since the reaction rate constant is temperature dependent, with a fixed concentration of scavenger, the scavenging time is in fact different for each temperature. Moreover, the spur lifetime (the time required for the changeover from non-homogeneous spur kinetics to homogeneous kinetics in the bulk solution) is an important aspect for the discussion of temperature dependent behaviors of *G*-value of water decomposition products. Based on irradiated Fricke dosimeter Monte-Carlo simulations, the spur lifetime was found to decrease monotonically from ~2.1×10^{-7} s at 25 °C to ~3.5×10^{-8} s at 350 °C (with an estimated uncertainty of about ±10 %)[12].

3.3 Reaction rate constants

The measurement of reaction rate constants is rather challenging, not only because there are several tens reactions (they should be well "separated" to determine) but also due to the rapid decay with increasing temperature. Nevertheless, some studies were devoted to reactivity at temperatures higher than 300 °C or even in SCW in the last decade. The results have demonstrated the unusual behaviors of rate constants at elevated temperatures. Some reactions follow well the linear relationship of Arrhenius equation, while many others exhibit non-Arrhenius behavior. As an example, Fig. 4 shows the Arrhenius plots for the reaction of 4,4′-bpy with e^-_{aq}. At 25 MPa, from room temperature to 350 °C, there is a fairly good linear relationship from which an activation energy of 19.6 kJ/mol is calculated. The inset figure shows the rate constant as a function of water density at 380 °C. Apparently there is a significant density effect on the rate constants.

3.4 Behaviors of solvated electron in alcohols at elevated temperatures

Figure 5 shows the transition energy at the absorption maximum plotted as a function of temperature for the solvated electron in some primary alcohols (methanol, ethanol, 1-propanol, 2-propanol, 1-butanol, 1-pentanol, 1-hexanol, and 1-octanol) and four poly-alcohols, ethane-1,2-diol (Eg), propane-1,2-diol (12PD), propane-1,3-diol (13PD), and propene-1,2,3-triol (Glycerol) that we investigated in recent years[13–20]. In general, by increasing the temperature, the decays become faster and most of the solvated electrons disappear within the electron pulse due

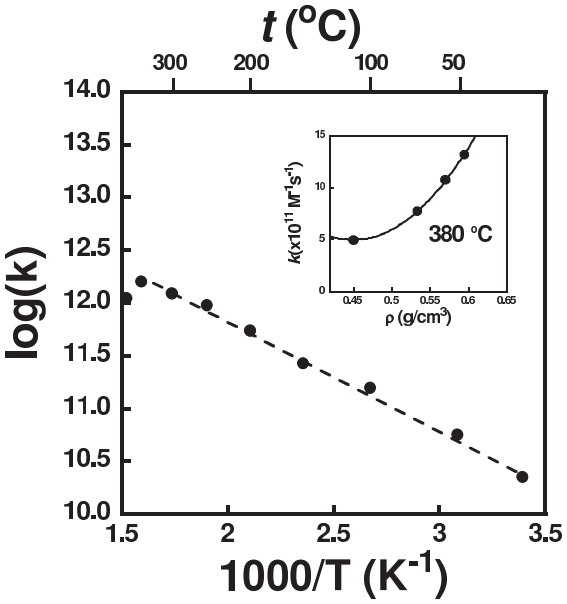

Figure 4. Arrhenius plots for the reaction of 4,4′-bpy with hydrated electron. Inset: Rate constant as a function of density at 380 °C.

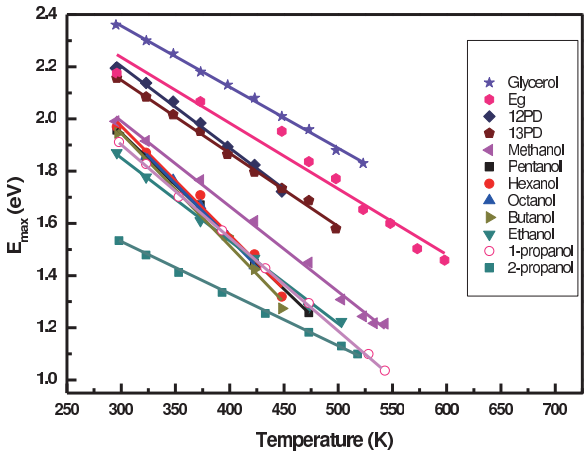

Figure 5. Transition energy at the absorption maximum as a function of temperature for the solvated electron in various alcohols.

to the geminate recombination. However, it can be clearly observed that the maximum of the solvated electron absorption band shifts to the longer wavelength with the temperature rise. For the primary alcohols (*n*-alcohols), the temperature coefficient increases with increasing chain length. For the alcohols with same chain length and OH numbers, temperature coefficient is larger for the symmetric alcohols than the asymmetric ones.

Very interestingly, for the solvated electron in poly-ols, the red-shift of the spectrum with increasing temperature corresponds very well with the spectral shift of electron solvation obtained by femtosecond laser photolysis, that is, higher temperature corresponds to shorter time. For example, in the case of glycerol, the spectra at 125, 100, and 75 °C agree fairly well with those at 100 fs, 3 ps, and 20 ps, respectively. The blue shift of the absorption spectrum of the electron during solvation in poly-ols is continuous and can be described by the temperature dependent absorption spectrum of the ground state solvated electron, suggesting that the blue shift is caused mostly by the thermal relaxation of the solvated electron.

4 Summary

Under sub- or supercritical conditions, the radiolytic yields of water decomposition products, the reaction rate constants and the spectral properties of transient species show significant difference from those of water at ambient condition or even at elevated temperatures below 300 °C. These properties are not only dependent on temperature but also greatly affected by water density in SCW, or in other words, they exhibit non-linear behaviors or even non-monotonic function with temperature at a fixed pressure. This would strongly suggest a re-consideration of current model of water radiolysis in nuclear reactors, especially for the future SCW reactors, where the temperature varies from 285 °C at the inlet to more than 550 °C at the outlet. On the other hand, these unusual behaviors are certainly related to the peculiar water properties and water structure of SCW such as dielectric constant, hydrogen bonding network, clustering, and density inhomogeneity, etc. This requires more fundamental studies on temperature effects of the electron solvation processes, the spur reaction processes and other more general chemical interests in these intriguing reaction media.

Acknowledgement

The author is very grateful to Prof. Y. Katsumura at the Univ. of Tokyo, Prof. Y. Muroya at Osaka Univ., Prof. M. Mostafavi at the Univ. Paris-Sud, Prof. J. P. Jay-Gerin at Sherbrooke Univ., Prof. Y. Hatano, and Prof. M. Uesaka, for their fruitful collaborations, scientific discussions, and encouragement. I'm also thankful to Dr. G. Wu, Dr. H. He, Dr. H. Fu, Dr. Z. Han, Dr. T. Miyazaki, Dr. S. Yamashita, Dr. Y. Kumagai, Dr. K. Hata, and many other researchers and students who have contributed to those related studies. I'd like to express his sincere thanks to Ms. S. Tokoro and Mr. T. Ueda for their kind helps all along.

References

1) E. J. Hart, J. W. Boag, J. Am. Chem. Soc., 84 (1962) 4090; E. J. Hart, J. W. Boag, Nature, 197 (1963) 45.
2) M. Lin, Y. Muroya, G. Baldacchino, Y. Katsumura, in "Recent Trends in Radiation Chemistry", eds. J. F. Wishart M. Rao, World Scientific Publishing Company, pp.255–277, 2010; M. Lin, Y. Katsumura, in "Charged Particle and Photon Interactions with Matter: Recent Advances, Applications, and Interfaces", eds. Y. Hatano, Y. Katsumura, A. Mozumder, Taylor and Francis Group, pp.401–424, 2011.
3) M. Mostafavi, M. Lin, G. Wu, Y. Katsumura, Y. Muroya, J. Phys. Chem. A, 106 (2002) 3123.
4) Y. Muroya, M. Lin, V. de Waele, Y. Hatano, Y. Katsumura, M. Mostafavi, J. Phys. Chem. Lett., 1 (2010) 331.
5) J. P. Jay-Gerin, M. Lin, Y. Katsumura, H. He, Y. Muroya, J. Meesungnoen, J. Chem. Phys., 129 (2008) 114511.
6) Y. Yan, M. Lin, Y. Katsumura, Y. Muroya, S. Yamashita, K. Hata, J. Meesungnoen, J. P. Jay-Gerin, Can. J. Chem., 88 (2010) 1026.
7) E. G. McRae, J. Phys. Chem., 61 (1957) 562.
8) M. Lin, Y. Katsumura, Y. Muroya, H. He, G. Wu, Z. Han, T. Miyazaki, H. Kudo, J. Phys. Chem. A, 108 (2004) 8287.
9) M. Lin, Y. Katsumura, H. He, Y. Muroya, Z. Han, T. Miyazaki, H. Kudo, J. Phys. Chem. A, 109 (2005) 2847.
10) M. Lin, Y. Katsumura, Y. Muroya, H. He, T. Miyazaki, D. Hiroishi, Radiat. Phys. Chem., 77

(2008) 1208.
11) Y. Muroya, S. Sanguanmith, J. Meesungnoen, M. Lin, Y. Yan, Y. Katsumura, J. P. Jay-Gerin, Phys. Chem. Chem. Phys., 14 (2012) 14325.
12) S. Sanguanmith, J. Meesungnoen, Y. Muroya, M. Lin, Y. Katsumura, J. P. Jay-Gerin, Phys. Chem. Chem. Phys., 14 (2012) 16731.
13) M. Mostafavi, M. Lin, H. He, Y. Muroya, Y. Katsumura, Phys. Lett., 384 (2004) 52.
14) I. Lampre, M. Lin, H. He, Z. Han, M. Mostafavi, Y. Katsumura, Chem. Phys. Lett., 402 (2005) 192.
15) Z. Han, Y. Katsumura, M. Lin, H. He, Y. Muroya, Chem. Phys. Lett., 404 (2005) 267.
16) M. Lin, M. Mostafavi, Y. Muroya, Z. Han, I. Lampre, Y. Katsumura, J. Phys. Chem. A, 110 (2006) 11404.
17) M. Lin, M. Mostafavi, Y. Muroya, I. Lampre, Y. Katsumura, Nucl. Sci. Tech., 18 (2007) 2.
18) Z. Han, Y. Katsumura, M. Lin, H. He, Y. Muroya, H. Kudo, Radiat. Phys. Chem., 77 (2008) 409.
19) M. Lin, H. Fu, I. Lampre, V. de Waele, Y. Muroya, Y. Yan, S. Yamashita, Y. Katsumura, M. Mostafavi, J. Phys. Chem. A, 113 (2009) 12193.
20) Y. Yan, M. Lin, Y. Katsumura, H. Fu, Y. Muroya., Radiat. Phys. Chem., 79 (2010) 1234.

Biography

Mingzhang Lin： M. Lin received his B.S. degree in Polymer Physics from the University of Science and Technology of China (USTC) in 1988 and his Ph.D. in Physical Chemistry from the University of Paris-Sud in 1996. He joined the Nuclear Engineering Research Laboratory (now Nuclear Professional School) of the University of Tokyo and worked as postdoc and research fellow from 2000 to 2007. Then he worked as a senior scientist at Japan Atomic Energy Agency before he moved to the USTC in 2012. He is now professor at the USTC and the Institute of Nuclear Energy Safety Technology, Chinese Academy of Sciences.